Power System Technology
ISSN:1000-3673

Received: 16-10-2025 Revised: 05-11-2025 Accepted: 06-12-2025

Particle Swarm-Optimized Artificial Neural Network for Non-Invasive Glucose Measurement and Hba1c Computation

Suma K V [1,*], Dharini Raghavan[2], Maya V Karki [3], Narayana Sharma [4], Gundu Rao [5]

[1,2,3] *Department of Electronics and Communication Engineering, Ramaiah Institute of Technology, India*
[4] *Photonics India Venture Private Limited, India*
[5] *University of Minnesota, Twin Cities, USA*
**Corresponding author: sumakv@msrit.edu*

Abstract:- Blood glucose is typically measured using invasive methods such as finger pricking, which although accurate are not suitable for frequent use as they cause extreme pain, and do not provide provisions for continuous glucose monitoring. Recent studies have proposed non-invasive glucometers that are based on scientific principles such as optical polarimetry, thermal emission, and electromagnetic approaches, but are expensive, highly sensitive to external noise and environmental variations, have low signal-to-noise ratio (SNR), and poor glucose selectivity. Although developments in Near-Infrared Spectroscopy (NIRS) have overcome these limitations to a certain extent, they do not produce reliable measurements due to large calibration errors that often result in incorrect glucose readings. In this paper, we propose a robust particle-swarm optimization-based artificial neural network for non-invasive continuous glucose monitoring using the principles of NIRS. We show that the PSO-ANN approach outperforms the traditional backpropagation algorithm used in ANN training and several other regression algorithms with the lowest error metrics: MAE- 1.01, MSE-2.16, RMSE-0.97, R^2-0.976 and modified R^2-0.973. The paper also provides insights into the circuit design, sensors used, hardware-software integration, and clinical validation alongside providing an overview of HbA1c computation. The accuracy and reliability of the proposed system are analysed using the Clarke Error Grid (CEG) with 93.9% of the obtained readings falling within zone A and 100% of the readings falling in the clinically accepted range (zones A and B). The paper also explores potential enhancements such as miniaturization of the prototype device for wearable applications and wireless connectivity.

Keywords: *Diabetes mellitus, non-invasive, near-infrared spectroscopy, calibration models, artificial neural network, particle swarm optimization.*

1. Introduction

Diabetes mellitus (DM) is a metabolic disease that occurs due to inefficient regulation of glucose levels in the body and is characterized by high glucose levels over a prolonged duration. According to a report by the International Diabetes Federation (IDF) [1], a total of 577 million individuals are currently affected by diabetes globally. According to WHO [2], diabetes is classified as one of the major non-communicable diseases (NCD) contributing to the highest death rate worldwide. It is also estimated that the percentage of individuals affected

Power System Technology
ISSN:1000-3673
Received: 16-10-2025 Revised: 05-11-2025 Accepted: 06-12-2025

with diabetes will continue to increase exponentially in the years to come [3,4]. Frequent monitoring of blood glucose levels contributes to effective diabetic health management that helps identify fluctuations or anomalies in glucose concentration and further helps avoid health complications. Although conventional glucose measuring devices are accurate, they are not suitable in the long run as they cause extreme pain, discomfort, and risk of infections. Alongside, the test strips are for single-time use and expensive, which limits their use to a maximum of 3 or 4 times a day. This on the other hand is not sufficient to keep track of an individual's diabetic health that needs continuous monitoring and analysis. Therefore, the development of non-invasive glucometers has garnered significant interest in recent years, aiming to provide a more convenient and user-friendly alternative for individuals with diabetes. Non-invasive methods can be broadly classified such as thermal, photo-acoustic, electro-chemical, electro-magnetic, optical, and biofluids-based approaches [5,6,7,8]. Among the various non-invasive techniques explored for glucose monitoring, Near Infrared Spectroscopy (NIRS) has emerged as a promising technology. NIRS utilizes the absorption and scattering properties of near-infrared light (wavelength in the range from 700 to 2500 nm) to obtain information about the molecular composition of biological tissues, including glucose concentrations. In this paper, a wavelength of 940 nm is selected that falls in the near-infrared region since glucose has a light absorption peak at this wavelength as well as the attenuation offered by other constituents of the blood like water, platelets, red blood cells, etc. is minimum at this wavelength [9]. This in turn helps to achieve a desired depth of penetration and the actual glucose concentration can be predicted.

Calibration of non-invasive glucometers is one of the most critical aspects that establishes a mapping between the absorbance of light and glucose concentration. This involves the application of Beer Lambert's law which states that the absorbance of light passing through a sample is directly proportional to the concentration of the absorbing substance and path length of the light wave that travels through the sample. This is achieved using an infrared transmitter that emits waves in the NIR spectroscopy which is passed through the measurement site (typically fingertip or earlobe) and a photo-detector captures the amount of light absorbed by the tissues. The current flowing through the photo-detector is then converted to a voltage value using an operational amplifier which is further used in regression analysis. In this work, we investigate a range of regression algorithms for estimating blood glucose concentration from a corresponding voltage value obtained from a photo-detector and an operational amplifier.

2. Related Work

Non-invasive glucometers are designed to measure glucose levels that can help accomplish continuous glucose monitoring in a painless, infection-risk-free, and low-cost manner causing no harm to human tissues. In contrast to invasive glucose measuring devices that adopt an

Power System Technology
ISSN:1000-3673
Received: 16-10-2025 Revised: 05-11-2025 Accepted: 06-12-2025

electro-chemical method where a chemical reaction between blood and glucose oxidase biosensors results in a corresponding glucose reading, non-invasive glucometers use scientific principles such as scattering of light and electromagnetic interference to get an estimate of blood glucose concentration. There are several other approaches including photoacoustic, thermal, electrochemical, and measurement using bio-fluids for non-invasive glucose measurement among which optical approaches have been widely adopted due to a range of advantages they offer.

2.1 Optical Approaches

Optical methods involved in non-invasive glucose measurement are based on the behavior of light waves when passed through blood and its constituents. Alongside NIRS [10], some of these approaches involve principles of Raman spectroscopy [11], diffuse reflectance spectroscopy [12], and time-resolved fluorescence [13]. When light passes through blood, different components absorb different amounts of light that result in absorption bands associated with each constituent of blood. Glucose has its absorption peaks situated in the mid-infrared region (2.5–50 μm) to the near-infrared region (0.7–5 μm). Apart from optical approaches, several other principles are adopted in non-invasive glucose measurement as described in [14,15,16].

2.2 Existing Implementations of Non-Invasive Glucometer

Although there are numerous approaches for non-invasive glucose measurements, certain limitations persist with each. While some of these approaches are not suitable for integration into portable devices, many of these approaches showcase low glucose sensitivity and are inefficient in noisy environments. Among the variety of approaches that exist, NIRS has emerged as a promising method for non-invasive glucose measurement that overcomes these limitations to a certain extent when integrated with robust signal processing and calibration algorithms. In [17], the authors propose a non-invasive glucose-measuring device integrated with multiple sensors for continuous monitoring of blood glucose levels. The multi-sensor device provides capabilities for monitoring and estimating glucose levels by estimating physiological changes including temperature, humidity, optical properties, and impedance spectroscopy at varying frequencies. Although the multi-sensor approach proposed in the study performs reasonably well, the device has a high RMSE that indicates higher possibilities of errors in glucose readings. In [18], the authors discuss different challenges associated with continuous glucose monitoring (CGM) and integrated sensors. In [19], a Raspberry Pi system is proposed that is interfaced with a camera for capturing images of the skin tissue when visible laser light passes through the surface of the skin. The blood glucose level is obtained by an Artificial Neural Network (ANN) that is modelled based on the amount of light absorbed and scattered by skin tissues. The prototype was tested on 8 volunteers and the readings were compared with glucose levels obtained from commercial glucometers. The authors of [20],

Power System Technology
ISSN:1000-3673
Received: 16-10-2025 Revised: 05-11-2025 Accepted: 06-12-2025

trained a range of machine learning models such as k Nearest Neighbors (kNN), Naive Bayes, Support Vector Machines, Random Forest, Decision Trees, Neural Networks, and a few regression algorithms for non-invasive blood glucose measurement. This work considers two different datasets namely: PIDD and iGLU, and the classification algorithms are evaluated based on different metrics such as accuracy, inference time, precision, recall, F1 score, and area under the curve (AUC) whereas the performance of the regression algorithms are measured based on metrics such as root mean squared error (RMSE) and mean absolute error (MAE). Among the algorithms that were tested, the Random Forest classifier produced the highest accuracy of 84%, recall of 68%, precision of 76%, and F1 score of 72% trained on the PIDD and the Decision Tree classifier showed the best performance with an accuracy of 70%, MAE score of 8%, RMSE score of 8.5% trained on the iGLU dataset. The authors of [21] propose a system that employs photoplethysmography (PPG) signals for non-invasive glucose estimation. The paper proposes a system that involves an optical sensor-based PPG signal acquisition system. The paper investigates various features associated with PPG signals using a single pulse analysis (SPA) technique for blood glucose estimation. The study involved 611 subjects and the PPG signals recorded spanned over 3 minutes each. Following data acquisition, the PPG signals are analyzed over different combinations of features including time domain features, frequency transformed features, and SPA. In [22], the authors propose a novel instrument based on near-infrared spectroscopy for probing human fingers that can also be used for non-invasive glucose measurement. Although the method is highly reliable, the complex mechanisms involved in it make it difficult for real-time deployment. Although several studies in the literature report accuracies over 95% with clinical reliability of blood glucose readings, most of the proposed devices have not been tested under variations in glucose concentration. They have not been extensively tested under OGTT and glucose loading tests and do not convey information about parameters such as HbA1c which are important indicators of diabetic health. To bridge the gap between the current literature and the actual consumer requirement, we propose an end-to-end non-invasive glucometer based on NIRS that is calibrated to produce blood glucose readings based on a particle swarm optimized artificial neural network (PSO-ANN). We rigorously test the device under glucose loading tests and OGTT alongside providing provisions to compute HbA1c values that provide an estimate of the average blood glucose levels for three months. Further, we also discuss the design of our prototype which is made compact and portable for easy integration and deployment onto clinical systems and hand-held devices for remote glucose monitoring.

Power System Technology
ISSN:1000-3673
Received: 16-10-2025 Revised: 05-11-2025 Accepted: 06-12-2025

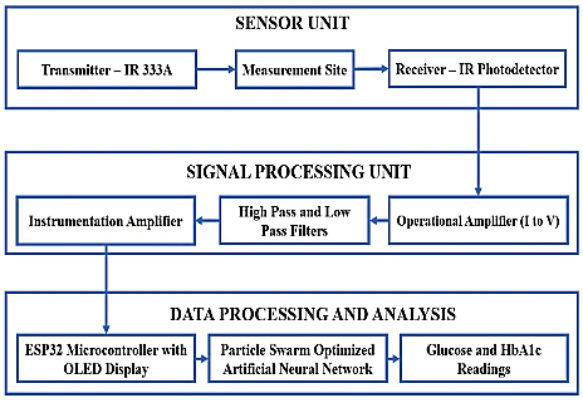

Fig.1. Overall Methodology

3. Overall Methodology

The end-to-end methodology of the non-invasive glucometer is depicted in Figure 1. Using the principle of Beer Lambert's law, the non-invasive glucometer essentially consists of three major blocks namely: sensor unit, signal processing unit, data processing, and analysis unit. Beer-Lambert's Law is a fundamental principle in spectroscopy that relates the absorption of light by a substance to its concentration. The sensor unit consists of an EverLight IR-333. A transmitter that emits infrared waves of wavelength 940 nm. This specific wavelength of 940 nm has maximum glucose sensitivity and the least attenuation offered by other constituents of blood and hence proves to be the most suitable wavelength in the NIR region for glucose measurement. The NIR waves emitted by the transmitter pass through the measurement site (fingertip) where light undergoes both absorption and scattering. The amount of light absorbed by the blood is measured by an Everlight phototransistor PT-333C that has peak sensitivity at 940 nm attenuation that the transmitted light wave suffers and the glucose concentration can thus be modelled. The photodetector measures this attenuation and resultant current flows through it which is further converted to a corresponding voltage value using an operational amplifier. The signal processing unit consists of an operational amplifier, filter circuits, and an instrumentation amplifier. The output voltage from the operational amplifier passes through a set of filter networks that consist of high-pass and low-pass filters with cutoff frequencies equal to 1.5 kHz and 2.2 kHz respectively. The filtered signal is then passed through an instrumentation amplifier with voltage gain equal to 101. The output voltage is fed to the data processing and analysis unit consisting of an ESP32 microcontroller integrated with an OLED unit for displaying corresponding glucose values. The microcontroller is programmed with the proposed PSO-ANN calibration algorithm which is described in Section 3.2. The algorithm is also designed to provide HbA1c values based on the measured blood glucose levels. The

Power System Technology
ISSN:1000-3673
Received: 16-10-2025 Revised: 05-11-2025 Accepted: 06-12-2025

subsequent sections provide an elaborate description of each module involved in the design of the non-invasive glucometer.

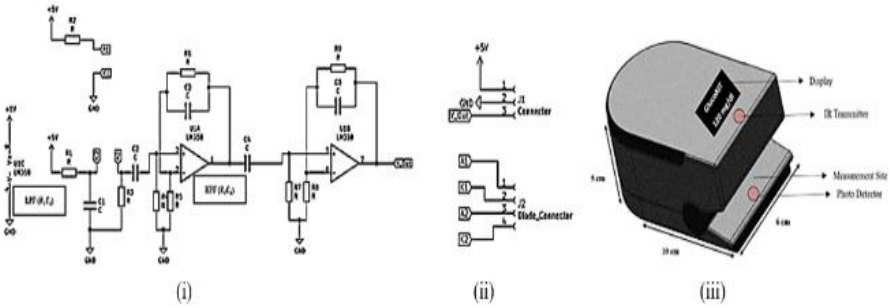

Fig 2: Non-invasive glucometer circuit design (i) glucometer circuit (ii) Connectors (iii) prototype design

Table 1: Performance comparison of different ANN architectures

Architecture (with 2 hidden layers)	Validation Error (RMSE)	Accuracy (%)
3-3-3-1	2.451	65.1
3-4-3-1	2.109	69.6
3-4-4-1	1.897	75.4
3-5-4-1	1.658	78.0
3-5-5-1	1.432	84.8
3-4-5-1	0.970	98.2
3-2-2-1	0.964	98.5
3-3-2-1	**0.942**	**98.9**

3.1 Sensor and Signal Processing Unit

The circuit employed in the proposed non-invasive glucometer is designed using a PCB design tool called KiCAD and is depicted in Figure 2. It broadly consists of the transmitter component and the receiver component where the receiver component further consists of filter networks and amplification units. The current at the output of the photodetector is converted to a corresponding voltage value using an operational amplifier network with load respectively. The LPF is connected to the cathode of the photodiode.

3.2 Artificial Neural Network (ANN) for Blood Glucose Calculation

A typical structure of an ANN is depicted in Figure 3 which consists of an input layer, one or more hidden layers, and an output layer.

Power System Technology
ISSN:1000-3673
Received: 16-10-2025 Revised: 05-11-2025 Accepted: 06-12-2025

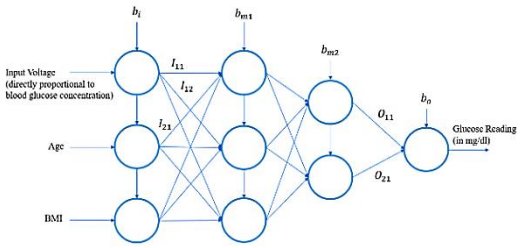

Fig 3: Structure of proposed ANN

The input features to the neural network are fed to the input layer which in our case is the output voltage, age and body mass index (BMI) of the subjects involved in this study. The weights assigned to each of these input features are updated by intermediate connections and weights in the hidden layer. Each layer has an associated activation function that computes the output of a particular layer which further serves as the input to the subsequent layers. We employ the sigmoid activation function in the intermediate layers that adjust the
weights of the intermediate layers and helps the weights propagate to the output layer.
To overcome the limitations associated with the traditional BP algorithm, we adopt an evolutionary optimization algorithm called the particle swarm optimization (PSO) which is depicted in Section 3.3.

3.3 Particle Swarm Optimization-based ANN

PSO is a population-based optimization algorithm that represents a group of particles moving in space looking for the best solution to a given problem [11]. In a S dimensional search space consisting of N randomly initialized particles in the population, each particle i in the swarm keeps track of the current position X_i, prior best position P_i and the current velocity V_i. Alongside the particles also keep track of the particle's best position P_g that is computed as a fitness value. Based on the value of the best position, each particle updates its current position and velocity given by Eq. 1 and Eq. 2 as depicted below.

$$V_{new} = \alpha V_i + a_1(P_i - X_i)rand() + a_2(P_g - X_i)rand() \quad (1)$$

$$X_{new} = X_i + V_{new} \quad (2)$$

where V_{new} denotes the new particle velocity, a_1 and a_2 are acceleration constants (weighting coefficients), α is the inertial weight, $rand()$ is a random function in the range [0,1]. In this study, the major objective of the PSO algorithm is to minimize the error between the predicted glucose value and the actual glucose value given a set of input features. In the following section, we describe the proposed prototype of the non-invasive glucometer with its constructional features.

3.4 Prototype Design of a Non-Invasive Glucometer

We propose a compact, portable, and cost-effective design of a non-invasive glucometer that has an arch-like structure with the OLED display mounted on the top surface whereas the transmitter and receiver LEDs are enclosed within small-circular flaps. The prototype designed using Autodesk Fusion 360 and 3D printed is depicted in Figure 2 (iii). **4. Experiments and Results**

Power System Technology
ISSN:1000-3673
Received: 16-10-2025 Revised: 05-11-2025 Accepted: 06-12-2025

4.1 Implementation Details of PSO-ANN

In this study, we design an ANN with three neurons in the input layer, four neurons in the first hidden layer, five neurons in the second hidden layer, and one output neuron representing the estimated glucose value. We performed multiple experiments varying the number of neurons in the hidden layer and the 3- 3-2-1 ANN architecture produced the most accurate results. This architecture involves a total of 17 weights to be optimized and in the PSO algorithm, we set the dimension of the search space to be 17. Table 1 depicts the performance comparison of different architectures of ANNs trained for 70 iterations each and the architecture with the least error and maximum accuracy is selected. The other major parameters in the PSO algorithm are the size of the population, acceleration constants, and inertial weight. We consider a population size of 25, acceleration constants $a1$, $a2$ as 2.76 and 2.34 respectively and the inertial weight α as 1.25. The variation of the root mean squared error (RMSE) of the neural network with different values of these parameters are depicted in Figures 4 (i), (ii), and Figure 5.

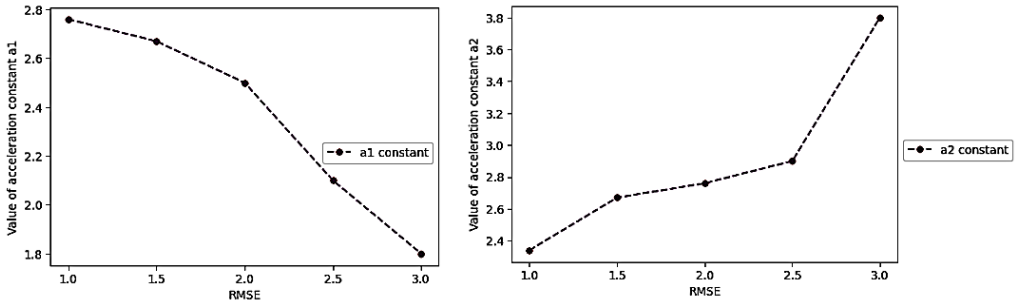

Fig 4: Variation of RMSE with acceleration constants (i) variation of RMSE with $a1$ (ii) variation of RMSE with $a2$

From Figure 4, it can be inferred that a value of 2.76 for $a1$ and 2.34 for $a2$ yield a minimum RMSE score of 1.1 and 0.98 respectively.

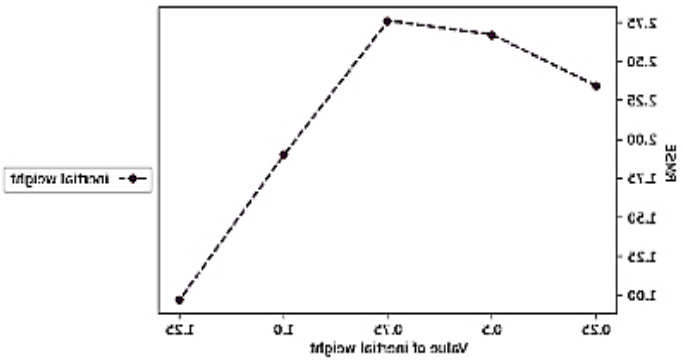

Fig 5: Variation of RMSE with inertial weight α (a value of α = 1.25 yields the minimum RMSE score of 0.95)

Power System Technology
ISSN:1000-3673
Received: 16-10-2025 Revised: 05-11-2025 Accepted: 06-12-2025

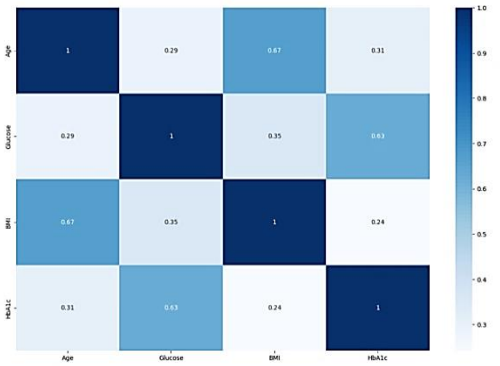

Fig 6: Correlation matrix for modelling blood glucose levels

4.2 Performance Analysis of Regression Algorithms for Non-Invasive Glucose Measurement

We analyze the performance of different regression algorithms and evaluate them based on several metrics such as Mean Absolute Error (MAE), Mean Squared Error (MSE), Root Mean Squared Error (RMSE), R^2 score and Modified R^2 score. Table 2 presents a performance comparison of several regression algorithms.

4.2.1 Evaluation Metrics for Regression Algorithms:

(i) Mean Absolute Error (MAE): It represents the absolute difference between the predicted values and the actual values averaged over the entire dataset which is mathematically represented as shown in Eq. 3. MAE represents the average of the residuals in the dataset.

$$MAE = \frac{1}{N}\sum_{i=1}^{N}|y_i - \hat{y}_i| \quad (3)$$

where N denotes the total number of samples in the dataset, y_i represents the actual value (ground truth) and $\hat{y}_i$ denotes the predicted value.

(ii) Mean Squared Error (MSE): It represents the difference between the squared values of the actual and the predicted samples averaged over the entire dataset. MSE measures the variance of the residuals in the dataset. The mathematical formulation of MSE is shown in Eq. 4.

$$MSE = \frac{1}{N}\sum_{i=1}^{N}(y_i - \hat{y}_i)^2 \quad (4)$$

(iii) Root Mean Squared Error (RMSE): It is the square root of the mean squared error and represents the standard deviation of the residuals in the dataset. RMSE is mathematically given by Eq. 5.

$$RMSE = \sqrt{\frac{1}{N}\sum_{i=1}^{N}(y_i - \hat{y}_i)^2} \quad (5)$$

(iv) R Squared and Adjusted R Squared Score: It represents the proportion of variance in the target variable explained by the independent variables. A regression model with a high R^2 score has a higher capability of modelling the relation between the dependent and independent

Power System Technology
ISSN:1000-3673
Received: 16-10-2025 Revised: 05-11-2025 Accepted: 06-12-2025

variables accurately. Modified R^2 the score is adjusted for the number of independent variables. R^2 score and Modified R^2 scores are given by Eq. 6 and Eq. 7 respectively.

$$R^2 = 1 - \frac{\sum(y_i - \hat{y}_i)^2}{\sum(y_i - \bar{y}_i)^2} \quad (6)$$

$$R_{modified}{}^2 = 1 - \frac{(1-R^2)(n-1)}{n-k-1} \quad (7)$$

where n is the number of samples in the dataset and k is the number of independent variables in the dataset.

Since RMSE and MSE are differentiable functions unlike MAE which is non-differentiable, the former are preferred metrics over the latter. Both R^2 score and RMSE quantify the performance of regression models and measure how well they model the relation between the dependent and independent variables. We perform a correlation analysis to visualize different parameters that contribute to the onset of diabetes. On analysis of the correlation heatmap as shown in Figure 6, we observe that blood glucose is significantly correlated to age and BMI with a correlation coefficient of 0.29 and 0.35 respectively.

Hence, for modelling the PSO-ANN calibration algorithm, we use age and BMI as input features alongside output voltage. We compare the RMSE variation of the PSO-ANN algorithm with traditional ANNs and it is observed that the slope of the error curve for the PSO-optimized ANN is 28.7% lower than traditional ANNs. Hence, the proposed PSO-ANN algorithm proves to have higher reliability in non-invasive glucose measurement. We perform a correlation analysis with the data collected to visualize different parameters that contribute to the onset of diabetes. Figure 6 depicts a correlation matrix that portrays the relationship between blood glucose levels and different parameters such as age, BMI, and HbA1c. On careful analysis, it is seen that blood glucose is significantly correlated to age and BMI with a correlation coefficient of 0.29 and 0.35 respectively. Hence, for modeling the PSO-ANN calibration algorithm, we use age and BMI as input features alongside output voltage.

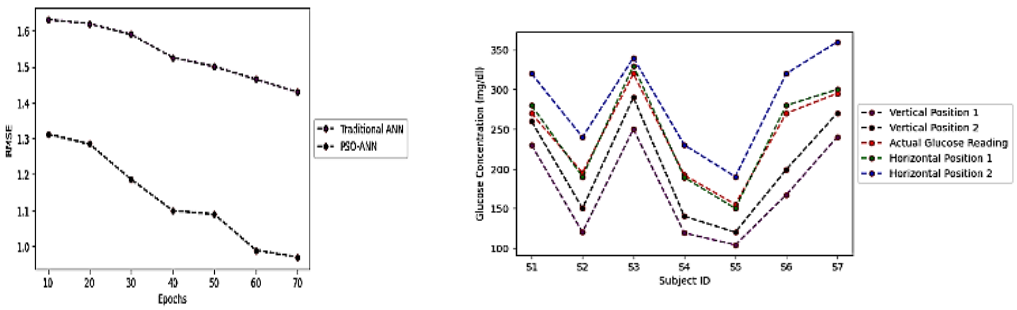

Fig 7: (i) RMSE variation of traditional ANN and PSO-ANN (ii) Variation of glucose concentration with different positions of fingertip

Figure 7 (i) depicts the RMSE variation of the PSO-ANN algorithm when compared against traditional ANNs. The slope of the error curve for the PSO optimized ANN is 28.7% lower than traditional ANNs. Hence, the proposed PSO-ANN algorithm proves to have higher reliability in non-invasive glucose measurement. Figure 7 (ii) presents the readings obtained for 7 subjects with different positions of the fingertip and the actual glucose reading for every

Power System Technology
ISSN:1000-3673
Received: 16-10-2025 Revised: 05-11-2025 Accepted: 06-12-2025

subject measured using a commercial glucometer. It is seen that horizontal position 1 provides highly reliable and accurate glucose readings that are extremely close to the actual glucose readings.

4.3 Glucose Loading and OGTT

In this study, we involved a total of 20 subjects belonging to the age group of 20 to 55 years who provided consent to participate in the glucose loading and random glucose tests. Out of the 20 subjects, 10 subjects participated in the glucose loading test and random glucose test, and the remaining 10 of them participated in HbA1c analysis. The entire experiment spanned for a total of 3 hours and we initially performed an oral glucose tolerance test (OGTT), where each subject's fasting glucose levels were measured. Each subject is asked to consume 5 g of glucose powder and their blood glucose levels are continuously monitored and measured at regular intervals of time. To analyze the variation of glucose levels in subjects with varying severity of diabetes, we considered cases of extreme DM, moderate DM, and Normal subjects. In the case of extreme DM, the blood glucose concentration, rises exponentially with time, whereas the rate of increase of glucose concentration is lower in moderate DM and normal conditions.
This analysis could serve as an initial point for health professionals to categorize the stage of DM in an individual. Table 3 provides a comparison of non-invasive glucose measured along with the commercial glucometer readings of the subjects who took part in the glucose loading test along with random glucose
measurement. The glucose loading test was primarily performed to analyze and test the response of the device under varying levels of glucose concentration. This experiment was also done to measure the accuracy and sensitivity of the device to different concentrations of blood glucose.

Table 3: Experimental results before glucose loading, after glucose loading and random measurement

ID	Subject Age (years)	Voltage (mV)	BMI	Before Glucose Loading		After Glucose Loading		Random Glucose	
				Non-invasive	Invasive	Non-invasive	Invasive	Non-invasive	Invasive
S1	51	380	22.2	89.2	87.0	141.1	143.0	129.0	131.0
S2	45	545	21.9	112.0	110.0	136.5	138.0	132.0	133.0
S3	20	368	18.9	118.2	120.0	118.3	117.0	118.0	117.0
S4	24	359	19.1	86.3	87.0	108.0	110.0	102.0	100.0
S5	38	568	23.4	133.8	132.0	131.0	132.0	130.0	129.0
S6	45	572	24.0	130.0	132.0	132.0	130.0	123.0	122.0
S7	31	507	22.7	116.9	118.0	119.1	118.0	102.0	103.0

Power System Technology
ISSN:1000-3673
Received: 16-10-2025 Revised: 05-11-2025 Accepted: 06-12-2025

S8	54	539	24.3	102.4	101.0	120.5	122.0	114.5	111.0
S9	23	371	18.3	109.3	110.0	120.9	117.0	107.0	105.0
S10	25	396	19.3	98.2	96.0	120.0	118.0	100.0	102.0

4.4 HbA1c Computation and Analysis

Hemoglobin A1c (HbA1c) is a crucial parameter where the average blood glucose levels over the past two to three months are measured. It is an essential marker in diabetes management as it provides valuable information about a person's long-term glucose control. Using the estimated blood glucose levels non-invasively, we compute HbA1c as shown in Eq. 8 (a standard provided by the American Diabetes Association). The actual and estimated HbA1c values from the proposed device are listed in Table 4.

$$HbA1c = \frac{Glucose_{est}+46.7}{28.7} \quad (8)$$

Table 4: Experimental results for HbA1c comparison

ID	Subject Age (years)	Non-Invasive Glucometer (mg/dl)	Commercial Glucometer (mg/dl)	HbA1c (Actual) (mg/dl)	HbA1c (Estimated) (mg/dl)
S1	52	159.0	161.0	5.8	6.0
S2	49	139.0	138.0	4.8	4.5
S3	22	121.0	120.0	4.2	4.4
S4	25	123.0	124.0	4.0	4.3
S5	36	148.0	145.0	5.1	5.0
S6	45	131.0	130.0	5.2	5.4
S7	32	152.0	153.0	6.1	6.2
S8	53	216.0	211.0	6.9	7.1
S9	21	97.0	95.0	4.2	4.0
S10	20	100.0	102.0	4.7	4.8

The goal of using the Clarke Error Grid is to ensure that most of the predicted glucose values fall into zones A and B, indicating accurate and clinically acceptable predictions. In this work, we obtain 100% of the estimated values to fall within Zones A and B with a total of 93.9% of the values falling in Zone A which is depicted in Figure 8.

Power System Technology
ISSN:1000-3673
Received: 16-10-2025 Revised: 05-11-2025 Accepted: 06-12-2025

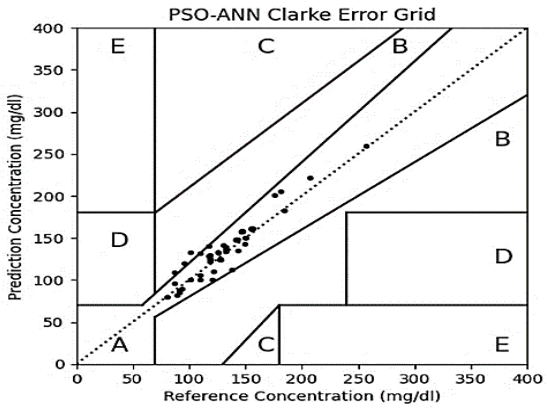

Fig 8: Clarke's Error Grid

5. Conclusion

In this paper, we present a non-invasive glucometer modelled using a PSO-ANN regression algorithm that has been extensively tested and analyzed under varying conditions of glucose concentrations. We extensively evaluate the performance of the proposed PSO-ANN algorithm and compare it with the existing as well as state-of-the-art algorithms for its accuracy and robustness. The proposed PSO-ANN algorithm with a 3-3-2-1 architecture achieves the highest accuracy of 98.9% and the best error measures listed as follows: MAE- 1.01, MSE-2.16, RMSE-0.942, R^2-0.976 and modified R^2-0.973. The RMSE of PSO-ANN converges to a global optimum much faster than the traditional BP-ANN as validated through our experiments. We provide an elaborate description of the circuit design, algorithmic specifications, and prototype design and provide a detailed explanation of the different experiments conducted to test the reliability of the non-invasive glucometer under different conditions. The proposed PSO-ANN algorithm outperforms the existing algorithms and we obtain 100% of the estimated glucose values to fall within the clinically acceptable regions. We also provide provisions for estimating HbA1c which most of the present devices lack and test the device under glucose loading and OGTT to provide robust performance under a range of conditions. In future, the device will be integrated with wearable devices and will also be made accessible via mobile devices.

ACKNOWLEDGEMENTS

Informed consent and patient details – Appropriate consent was obtained from the subjects involved in this study. The consent forms are available upon request. The study does not reveal the personal identity of the subjects. To preserve anonymity, we use unique IDs to refer to subjects.

Declaration of competing interest – The authors declare that they have NO competing interests in the execution of this work.

Funding – This work is financially supported by Photonics India Ventures Private Limited, India.

Power System Technology
ISSN:1000-3673
Received: 16-10-2025 Revised: 05-11-2025 Accepted: 06-12-2025

REFERENCES

1. IDF Diabetes Atlas. Available online: https://diabetesatlas.org/atlas/tenth-edition/
2. World Health Organization Noncommunicable Diseases, 2022. Available online: https://www.who.int/news-room/fact-sheets/detail/noncommunicable-diseases
3. Siddiqui S.A., Zhang Y., Lloret J., Song H., Obradovic Z. Pain-Free Blood Glucose Monitoring Using Wearable Sensors: Recent Advancements and Future Prospects. IEEE Rev. Biomed. Eng. 2018; 11:21–35. doi: 10.1109/RBME.2018.2822301
4. American Diabetes Association Diagnosis and Classification of Diabetes Mellitus. Diabetes Care. 2007; 30: S42–S47. doi: 10.2337/dc07-S042
5. Tang L., Chang S.J., Chen C.-J., Liu J.-T. Non-Invasive Blood Glucose Monitoring Technology: A Review. Sensors. 2020; 20:6925. doi: 10.3390/s20236925
6. Bolla A.S., Priefer R. Blood glucose monitoring- an overview of current and future non-invasive devices. Diabetes Metab. Syndr. Clin. Res. Rev. 2020; 14:739–751. doi: 10.1016/j.dsx.2020.05.016
7. Zhang R., Liu S., Jin H., Luo Y., Zheng Z., Gao F., Zheng Y. Noninvasive Electromagnetic Wave Sensing of Glucose. Sensors. 2019; 19:1151. doi: 10.3390/s19051151
8. Geng Z., Tang F., Ding Y., Li S., Wang X. Non-invasive glucose continuous glucose monitoring using a multisensor based glucometer and time series analysis. Sci. Rep. 2017; 7:12650. doi: 10.1038/s41598-017-13018-7
9. Cozzolino D. The Ability of Near Infrared (NIR) Spectroscopy to Predict Functional Properties in Foods: Challenges and Opportunities. Molecules. 2021; 26:6981. doi: 10.3390/molecules26226981
10. Garg, Saurabh & Patra, Karali & Pal, Surjya. (2014). Particle Swarm Optimization of a Neural Network Model in a Machining Process. Sadhana. 39. 10.1007/s12046-014-0244-7
11. Auer, B.M.; Skinner, J.L. IR and Raman spectra of liquid water: Theory and interpretation. J. Chem. Phys. 2008, 128, 224511
12. Malin, S F et al. “Noninvasive prediction of glucose by near-infrared diffuse reflectance spectroscopy.” Clinical chemistry vol. 45,9 (1999): 1651-8
13. Tang L, Chang SJ, Chen CJ, Liu JT. Non-Invasive Blood Glucose Monitoring Technology: A Review. Sensors (Basel). 2020 Dec 4;20(23):6925. doi: 10.3390/s20236925. PMID: 33291519; PMCID: PMC7731259
14. Boerio-Goates, J. Heat-capacity measurements and thermodynamic functions of crystalline α-D-glucose at temperatures from 10 K to 340 K. J. Chem. Thermodyn. 1991, 23, 403–409
15. V. Turgul and I. Kale, "Characterization of the complex permittivity of glucose/water solutions for noninvasive RF/Microwave blood glucose sensing," 2016 IEEE International Instrumentation and Measurement Technology Conference Proceedings, Taipei, Taiwan, 2016, pp. 1-5, doi: 10.1109/I2MTC.2016.7520546
16. Shokrekhodaei M, Quinones S. Review of Non-Invasive Glucose Sensing Techniques: Optical, Electrical and Breath Acetone. Sensors. 2020; 20(5):1251. https://doi.org/10.3390/s20051251
17. Geng, Z., Tang, F., Ding, Y. et al. Noninvasive Continuous Glucose Monitoring Using a Multisensor-Based Glucometer and Time Series Analysis. Sci Rep 7, 12650 (2017). https://doi.org/10.1038/s41598-017-13018-7

Power System Technology
ISSN:1000-3673
Received: 16-10-2025 Revised: 05-11-2025 Accepted: 06-12-2025

18. Rodbard D. Continuous Glucose Monitoring: A Review of Successes, Challenges, and Opportunities. Diabetes Technol Ther. 2016 Feb;18 Suppl 2(Suppl 2):S3-S13. doi: 10.1089/dia.2015.0417. PMID: 26784127; PMCID: PMC4717493
19. Valero M, Pola P, Falaiye O, Ingram KH, Zhao L, Shahriar H, Ahamed SI. Development of a Noninvasive Blood Glucose Monitoring System Prototype: Pilot Study. JMIR Form Res. 2022 Aug 26;6(8): e38664. doi: 10.2196/38664. PMID: 36018623; PMCID: PMC9463623
20. Agrawal, Harshita et al. "Machine learning models for non-invasive glucose measurement: towards diabetes management in smart healthcare." Health and technology vol. 12,5 (2022): 955-970. doi:10.1007/s12553-022-00690-7
21. Habbu, S., Dale, M. & Ghongade, R. Estimation of blood glucose by non-invasive method using photoplethysmography. Sādhanā 44, 135 (2019). https://doi.org/10.1007/s12046-019-1118-9
22. Chaiken, J. et al. Instrument for near infrared emission spectroscopic probing of human fingertips in vivo. Review of Scientific Instruments 81, 034301 (2010)